Upregulation of cortico-cerebellar functional connectivity after motor learning

Saeid Mehrkanoon * [1], Tjeerd W Boonstra* [2,3], Michael Breakspear[3,4], Mark Hinder[1], and Jeffery J. Summers[1,5]

[1]School of Medicine, Human Motor Control Laboratory, University of Tasmania, Private Bag 51, Hobart TAS 7001, Australia
[2]Black Dog Institute, University of New South Wales, Randwick, Sydney NSW 2052, Australia
[3]QIMR Berghofer Medical Research Institute, Brisbane QLD 4006 Australia
[4]Metro North Mental Health Service, Brisbane QLD 4006 Australia
[5]Research Institute for Sport and Exercise Sciences, Liverpool John Moores University, Liverpool, Merseyside L3 5UA, UK

*Corresponding authors, Saeid Mehrkanoon and Tjeerd W Boonstra, contributed equally to this work. Emails: smehrkanoon@gmail.com / t.boonstra@unsw.edu.au

Abstract

Interactions between the cerebellum and primary motor cortex are crucial for the acquisition of new motor skills. Recent neuroimaging studies indicate that learning motor skills is associated with subsequent modulation of resting-state functional connectivity in the cerebellar and cerebral cortices. The neuronal processes underlying the motor-learning induced plasticity are not well understood. Here, we investigate changes in functional connectivity in source-reconstructed electroencephalography (EEG) following the performance of a single session of a dynamic force task in twenty young adults. Source activity was reconstructed in 112 regions of interest (ROIs) and the functional connectivity between all ROIs was estimated using imaginary part of the coherence. Significant changes in resting-state connectivity were assessed using partial least squares (PLS). We found that subjects adapted their motor performance during the training session and showed improved accuracy but with slower movement times. A number of connections were significantly upregulated after motor training, principally involving connections within the cerebellum and between the cerebellum and motor cortex. Increased connectivity was confined to specific frequency ranges in the mu and beta bands. Post-hoc analysis of the phase spectra of these cerebellar and cortico-cerebellar connections revealed an increased phase-lag between motor cortical and cerebellar activity following motor practice. These findings show a reorganization of intrinsic cortico-cerebellar connectivity related to motor adaption and demonstrate the potential of EEG connectivity analysis in source-space to reveal the neuronal processes that underpin neural plasticity.

Keywords: Neural plasticity, intrinsic connectivity, motor learning, EEG source analysis, Cerebellum

1 Introduction

Neural plasticity is the ability of the brain to adapt its intrinsic functional organization to environmental changes and pressures, physiologic modifications and experiences (Pascual-Leone et al., 2005). Motor skill learning is a paradigmatic example of neural plasticity (Karni et al., 1995; Doyon and Benali, 2005; Halsband and Lange, 2006; Hikosaka et al., 2002; Sanes and Donoghue, 2000). Analogous to perceptual learning, the acquisition of new motor skills advances through two distinct stages: A single session improvement that can be induced by a limited number of trials, and subsequent slowly evolving, post-training incremental performance gains (Karni et al., 1998; Pascual-Leone et al., 2005; Luft and Buitrago, 2005; Doyon and Benali, 2005). In many instances, most gains in performance evolve in a latent manner not during training, but rather after training has ceased. The latent phase in human skill learning is thought to reflect a process of consolidation of experience-dependent changes in the cortex that are triggered by training, but continue to evolve thereafter (Karni and Sagi, 1993). Fast (single session) and slow (multi-session) learning processes are thought to involve distinct neural processes: dis-inhibition of existing connections within neural populations may induce changes on a short timescale, whereas structural modifications of connections and synapses may subserve slow learning and memory consolidation (Karni et al., 1998; Dudai, 2004; Dayan and Cohen, 2011).

Neuroimaging studies have investigated the neural substrates of these two phases of motor learning (Ungerleider et al., 2002; Kelly and Garavan, 2005; Tomassini et al., 2011; Krakauer and Mazzoni, 2011). Fast learning of sequential motor tasks modulates regional brain activity in the dorsolateral prefrontal cortex (DLPFC), primary motor cortex (M1) and pre supplementary motor area (preSMA) (Floyer-Lea and Matthews, 2005; Sakai et al., 1999) − which show decreased activation as learning progresses − and in the premotor cortex, supplementary motor area (SMA), parietal regions, striatum and the cerebellum − which show increased activation with learning (Grafton et al., 2002; Honda et al., 1998; Floyer-Lea and Matthews, 2005). M1 is one of the key brain regions involved in fast motor learning.

Likewise, slow learning − reflected by improved motor performance over multiple training sessions − is associated with increased activation in neuronal populations in M1 (Floyer-Lea and Matthews, 2005), primary somatosensory cortex (Floyer-Lea and Matthews, 2005), SMA (Lehéricy et al., 2005), putamen (Lehéricy et al., 2005; Floyer-Lea and Matthews, 2005), premotor cortex, supplementary motor area, parietal regions, and the cerebellum (Grafton et al., 2002; Floyer-Lea and Matthews, 2005), as well as an increase of gray matter in the supplementary motor area (Hamzei et al., 2012).

It is hence apparent that different parts of the distributed motor system, including subcortical structures such as the cerebellum and basal ganglia, are associated with motor skill learning (Karni et al., 1998; Galea et al., 2011). Therefore, understanding the functional role of multiple brain regions in motor learning requires investigation of distributed brain networks and connectivity patterns. Task-driven functional connectivity (Coynel et al., 2010) and effective connectivity (Ma et al., 2011; Tzvi et al., 2014) have indicated changes in the connections between M1 and the cerebellum during motor learning (Raymond et al., 1996; Inoue et al., 2000; Della-Maggiore et al., 2009). Alternatively, cortico-cerebellar connectivity has been indirectly assessed by evaluating changes in somatosensory evoked potentials (SEP) or motor evoked potentials (MEP) (Haavik and Murphy, 2013; Andrew et al., 2015; Baarbé et al., 2014). Recent resting-state fMRI studies revealed increased functional connectivity in cortical and subcortical regions after a short course of motor learning (Vahdat et al., 2011; Ma et al., 2011; Taubert et al., 2011; Tung et al., 2013; Sami et al., 2014). These findings further emphasise the involvement of the cerebellum in motor control and the consolidation of motor memory (Raymond et al., 1996; Inoue et al., 2000; Della-Maggiore et al., 2009).

Because of their superior temporal resolution, connectivity analysis of MEG and EEG data may provide additional information about the neuronal processes underpinning the changes in intrinsic connectivity following motor skill learning. Several MEG studies have shown changes in beta-band synchronization in the motor cortex during motor learning, reflecting a modulation in cortical excitability (Boonstra et al., 2007; Houweling et al., 2008; Pollok

et al., 2014). However, few studies have investigated connectivity changes in the distributed motor system using EEG or MEG. Motor-related changes in beta-band coherence have been observed in surface EEG (Deeny et al., 2009; Tropini et al., 2011). Coherence within the primary motor area in resting-state EEG has been used to predict subsequent motor acquisition in single session motor skill learning (Wu et al., 2014). Recent studies have shown that connectivity analysis of source-reconstructed MEG and EEG permits a better comparison to functional connectivity in fMRI data than sensor-based analyses (Mantini et al., 2007; Brookes et al., 2011; Mehrkanoon et al., 2014c). The ability to detect robust resting-state networks in source-reconstructed MEG and EEG suggests that this approach may also be sensitive to changes in intrinsic connectivity induced by motor learning. We hence performed source connectivity analysis in resting-state EEG recorded directly before and after a single session of motor skill learning. Given the prior results in fMRI connectivity analysis, we hypothesised that motor training would change the functional connectivity in the distributed motor system, in particular between the cerebellum and motor cortex. To examine this hypothesis, we compared whole-brain resting-state connectivity in source-reconstructed EEG before and after motor training and studied changes in intrinsic connectivity. By examining the frequency, phase and temporal information of resting-state coherence we sought to further elucidate the neuronal processes involved in neural plasticity during motor learning.

2 Materials and Methods

2.1 *Participants*

Twenty healthy right-handed adults (age: 21.3±1.8 years; 10 males) participated as volunteers in this study. The Human Research Ethics Committee of the University of Tasmania approved the protocol. All participants gave their informed consent according to National Health and Medical Research Council guidelines.

2.2 *Experimental design*

We compared intrinsic connectivity in source-reconstructed EEG before and after motor learning. For motor skill acquisition, we used a simple motor task in which participants were required to make a transition between two force levels as fast and accurately as possible. In a previous study we have shown a reorganization in corticomuscular coherence when participants make an overshoot when reaching the second target (Mehrkanoon et al., 2014b). Here we investigated how movement accuracy changes during a single session of motor training and compared cortico-cortical and cortico-cerebellar coherence during resting-state pre and post motor training. The task design involved three consecutive sessions: 1) an initial 10-minute resting-state session, 2) 20 motor skill training trials, and 3) a further 10 minutes of resting-state.

Participants were seated in a light- and sound-attenuated room with their right hand on a flat panel and their forearm supported. In the resting-state conditions, participants were instructed to relax with eyes closed and refrain from falling asleep. During the motor training session, participants were required to generate force by using their index finger and thumb (i.e. a pincer grip) against a force sensor (Figure 1C). Participants received visual feedback of the exerted force and were instructed to keep their force within pre-defined force intervals (target 1: $0.7-1.1$N, target 2: $1.9-2.3$N) displayed on a computer screen (Figure 1A). At the start of each trial, participants had to move the cursor into target 1 and keep it in the middle of targets until they perceived an auditory stimulus (a 1-s tone at 500 Hz). Once the stimulus was finished, participants had to move the cursor into target 2 as quickly as possible by increasing the exerted force and the keep it in the middle of target 2 until the end of the trial. The auditory stimulus was presented after a variable time interval ($9-11$ s) from the onset of the trial. The movement trajectory from target 1 to 2 was used to quantify motor performance.

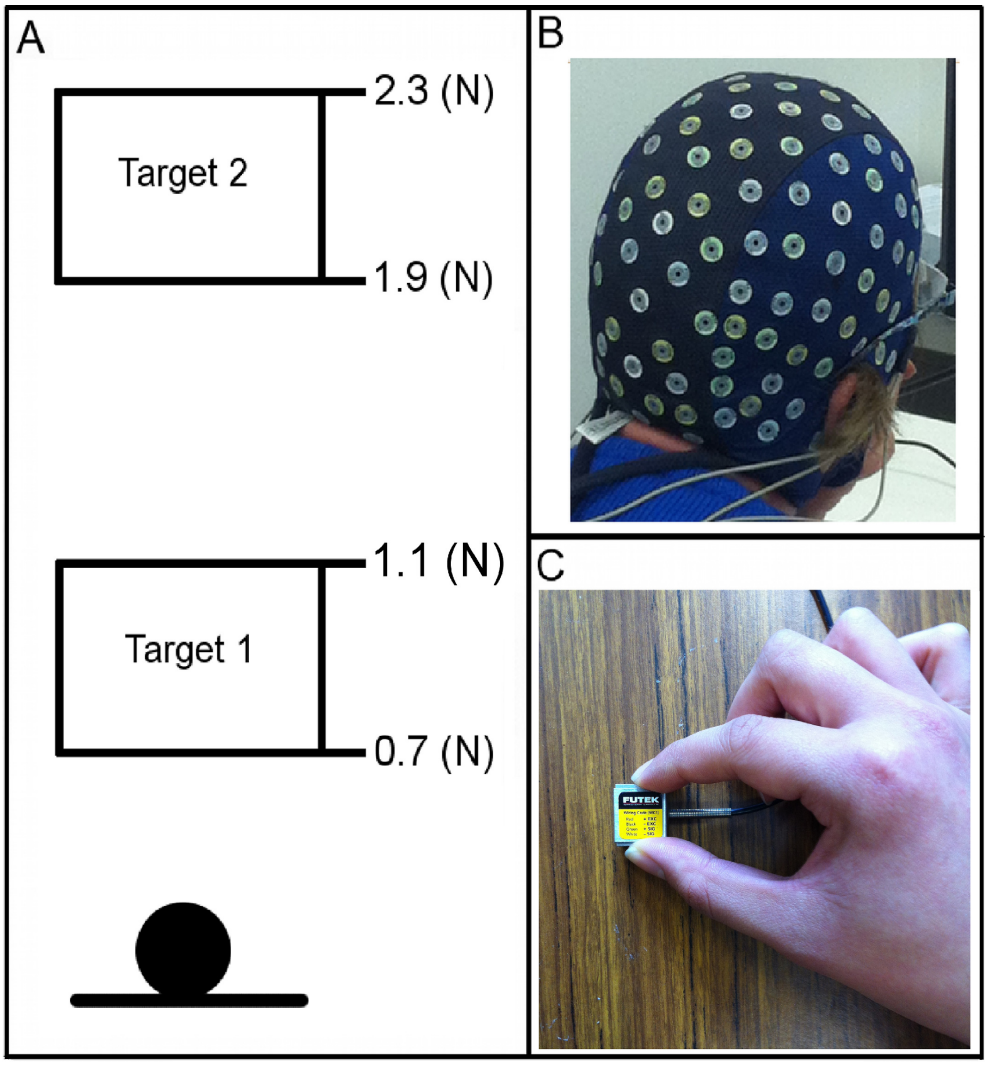

Figure 1: Task design. A) Diagram of the two force targets. B) Participant with an EEG cap. C) The force transducer. Subjects exerted force by using the index finger and thumb against the force sensor.

2.3 *Data acquisition*

A force sensor (LSB200 L2357, JR S-Beam load cell, FUTEK, California, USA) was used to measure the force exerted by the participant. The load cell was calibrated for every participant before the experiment. Participants were instructed to exert force against the load cell by using their index finger and thumb (Figure 1C). The force signal was amplified (SCG110, Strain Gage Amplifier, FUTEK, California, USA) and digitized at 1 kHz (NI USB-6259 BNC, National Instruments, Austin, Texas). 64 channel surface EEG was continuously acquired during the entire experiment (Figure 1B) from a 72 channel DC-amplifier during the entire 30-minute session (i.e. 10-minute resting-state, 20 trials of a motor task practice, and 10-minute resting-state) using an ANT Neuro waveguard EEG cap. EEG electrodes were arranged according to the international 10-20 system. Two additional channels were used for the electrooculography. All data were recorded at a sampling rate of 2048 Hz, and referenced against an electrode centered on the midline between Fz and Cz. The impedances of all electrodes were kept below 5 kΩ. EEG data were band-pass filtered (0.5$-$80 Hz). Independent component analysis (InfoMax) was used to identify and remove cardiac, ocular and muscular artifacts (Cardoso, 1997). The resulting EEG signals were then down-sampled to 500 Hz prior to further analyses.

2.4 *Behavioural data analysis*

We assessed motor performance by quantifying the speed and accuracy of the force trajectories between the two force targets. For each trial, the start of the trajectory from target 1 to 2 was defined as the last flection point of force trajectory before leaving target 1. Similarly, the endpoint was defined as the first flection point of force trajectory when reaching target 2. Movement duration was then defined as the time difference between the start and endpoint of the force trajectory. The movement error was defined as the force difference between the endpoint of the force trajectory and the middle of target 2 (2.1 N). This movement error hence corresponds to either an overshoot or an undershoot. We also quantified the interaction between speed and accuracy by fitting an exponential function to the movement-error

versus movement-duration trade-off across the 20 participants given by:

$$e = \frac{1}{1 + a\ \exp(b\tau)}\ , \tag{1}$$

where e denotes the movement error, a is a scaling parameter, b is the tuning parameter, and τ is the movement duration. In particular, the skill parameter, a, can be derived from Eq.(1) as $a = \frac{1-e}{e(\exp(b\tau))}$, where '$1 - e$' denotes the movement accuracy (Reis et al., 2009). We used a nonlinear least squares technique to estimate the skill parameter, a, and tuning parameter, b.

2.5 *EEG data analysis*

Functional connectivity analysis was performed on data from reconstructed cortical and cerebellar sources. To this end, an EEG source reconstruction approach was used to estimate cortical oscillations in the gray matter. Time−frequency coherence was estimated between all source combinations in two conditions: Pre (before motor training) and post (after motor training) resting-state. We compared the pre and post resting-state connectivity using a multivariate statistical approach to reveal the connections that showed a significant change in the intrinsic functional connectivity. Each of these steps, depicted schematically in Figure 2, is now defined in greater detail.

2.5.1 *Source reconstruction*

Analyses of the acquired EEG analysis were undertaken using a combination of publically available and in-house programs written in MATLAB (The Mathworks, Natick, MA). We used independent component decomposition (InfoMax ICA) to remove electro-occulograph (EOG) and electromyograph (EMG) artifacts from band-pass filtered EEG. For each participant, artifact-free EEG was down-sampled at 512 Hz before source reconstruction. We then employed the standard Low Resolution Electrical Tomography (sLORETA) algorithm to estimate source signals (Pascual-Marqui, 2002) computed by a Locally Spherical Model with Anatomical Constraints (LSMAC) (`brainmapping.unige.ch/cartool` Brunet et al.

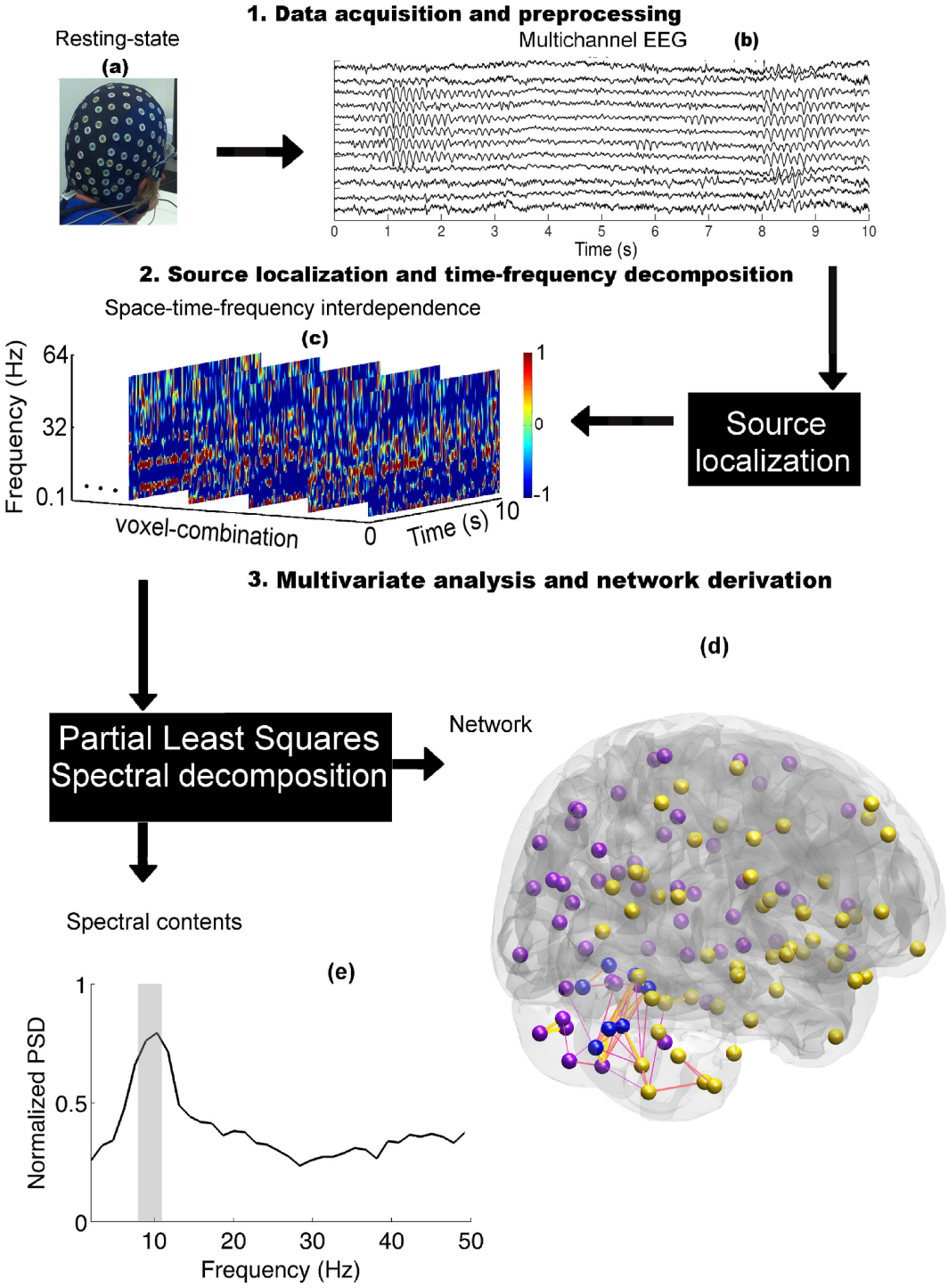

Figure 2: Construction of pre-post resting-state cortical networks. Top row: a) EEG data were acquired, b) preprocessed, artifact corrected and source reconstructed, and c) assessed pair-wise for time-frequency coherence. Resulting time-frequency spectra were concatenated (across subjects) and analyzed by using a multivariate partial least square analysis, d) Resting-state network constructed from an eigenvector derived from the PLS analysis, and e) spectral content of the network with a peak at significant carrier frequency 10 Hz.

(2011)) and the standard MNI152 brain template for all subjects. The LSMAC model does not require the estimation of a best-fitting sphere, but instead uses the realistic head shape and local estimates for the thickness of scalp, skull and brain underneath each local electrode. A total of 5400 solution points (henceforth referred to as voxels) were regularly distributed within the gray matter of the cortex and cerebellum. The forward model was solved by an analytical solution using a 3-layer conductor model. The source-space was subdivided into 112 anatomically defined regions of interest (ROIs) according to the macroscopic anatomical parcellation of the MNI template using the Automated Anatomic Labelling (AAL) map (Mazziotta et al., 2001). In CARTOOL (Brunet et al., 2011), four regions in the cerebellum have been merged: L-Cerebellum 4 and 5 (2 ROIs merged), R-Cerebellum 4 and 5 (2 ROIs merged), Vermis 1 and 2 (2 ROIs merged), and Vermis 4 and 5 (2 ROIs merged). Hence, 112 AAL regions were analyzed instead of the original 116 of the AAL atlas. On average, each ROI consisted of about 50 voxels. From these voxels we then determined one voxel per region that has the minimum average Euclidean distance to the rest of voxels in that brain region, the so-called centroid voxel. We then applied PCA to each of the centroid voxels separately, i.e., PCA to the "X, Y, and Z" components of a voxels time-series, to extract the orientation of the source-dipole dynamics within each ROI. The first PCA component (i.e., the first PCA projection) estimated from a single centroid voxel time-series was then used for further analysis. This is similar to the approach described by Hipp et al. (2012); Mehrkanoon et al. (2014c).

2.5.2 *Functional connectivity analysis*

We then computed functional connectivity between all voxel pairs using time-frequency coherence (Mehrkanoon et al., 2013, 2014a). Time-frequency coherence quantifies linear correlations between two observations, $\{x_t\}_{t=1}^{N}$ and $\{y_t\}_{t=1}^{N}$, as a function of time t and frequency f. Let $x(t)$ and $y(t)$ be two voxels time-series acquired from two given ROIs. The linear

correlation between these two voxels time-series is given by

$$\widehat{\Gamma}_{xy}(t,f) = \frac{S\left\{\hat{P}_{xy}(t,f)\right\}}{\sqrt{S\left\{\hat{P}_{xx}(t,f)\right\} S\left\{\hat{P}_{yy}(t,f)\right\}}} \quad t = 1, 2, ..., N \ , \tag{2}$$

where $\hat{P}_{xy}(t,f)$ denotes the Fourier cross-spectral density (CSD) estimate between signals $x(t)$ and $y(t)$, and $\hat{P}_{xx}(t,f)$ the power spectral density (PSD) estimate. Fourier based spectral decomposition was performed by using a unit power Hamming window of 1 s duration. The smoothing operator $S\{.\}$ used in this analysis is given by

$$K(t,f) = \exp\left(-\left(\frac{t^2}{2\sigma_t^2} + \frac{f^2}{2\sigma_f^2}\right)\right), \tag{3}$$

where $\sigma_t = 0.75$ s and $\sigma_f = 1.5$ Hz denote the time and frequency widths of the Gaussian kernel. Smoothing was implemented by convolving the kernel $K(t,f)$ with the time-frequency interdependence measures to improve the reliability of the coherency estimate (Mehrkanoon et al., 2013). Complex-valued time-frequency coherency was estimated between all voxel pairs − the total number of voxel combinations for 112 voxels is 6216 − producing a multidimensional time-frequency functional connectivity array (i.e. time × frequency × voxel combinations) for the pre- and post- resting-state conditions for all 20 subjects.

2.6 *Statistical analysis*

Multivariate statistical analysis was used to compare the connectivity arrays pre and post motor learning. Partial least squares (PLS) regression is a statistical tool that finds a linear regression model by projecting the independent and dependent variables to a new space that is rank ordered by the percent covariance explained. That is, PLS decomposes the original data into orthogonal modes that account for that part of the covariance structure that correlates with a specified design matrix (Geladi and Kowalski, 1986; McIntosh and Lobaugh, 2004; Langdon et al., 2011; Krishnan et al., 2011) (see also Eqs.(4a-c)). Here we use a design contrast as independent variable. In particular, a simple contrast between pre and post was

defined and regressed against the multivariate connectivity arrays. As the dependent variable we took the imaginary part of the complex-valued coherence in order to minimize the effect of volume conduction on the estimation of true functional connectivity (Nolte et al., 2004; Mehrkanoon et al., 2014a). Using only the imaginary part reduces the effect of source leakage on functional connectivity, as volume conduction (and hence source leakage) results in spurious correlations with a zero time (and phase) lag (see also Nolte et al. (2004); Hassan et al. (2014)).

To conduct PLS at the group level, the imaginary part of time-frequency coherence was first averaged across time (Eq.(4a)), yielding the coherence spectra as a function of frequency, voxel combinations, and number of subjects for all pre and post conditions. To implement the contrast, the pre-training coherence spectra were subtracted from post-training coherence spectra and then averaged across subjects, yielding grand-average group-level functional connectivity spectra as a function of frequency and voxel combinations (Eqs.(4b),(4c)). The resulting matrix was decomposed by the singular value decomposition into orthogonal components consisting of the singular values, $\mathbf{S}$ (Eq.(4d)), the latent variable (Eq.(4e)) (here frequency spectra obtained from the projection of the contrasted connectivity array), and the corresponding weights (or the left singular vectors, $\mathbf{U}$, which are the eigenvectors of the covariance matrix of $\mathbf{D}$) (Eq.(4d)).

$$\overline{\widehat{\Gamma}}_{i_{\text{pre}}}(f,m) = \frac{1}{N}\sum_{t=1}^{N} \Im\Big\{\widehat{\Gamma}^{m}_{i_{\text{pre}}}(t,f)\Big\}, \tag{4a}$$

$$\mathbf{D}_i(f,m) = \overline{\widehat{\Gamma}}_{i_{\text{post}}}(f,m) - \overline{\widehat{\Gamma}}_{i_{\text{pre}}}(f,m), \quad i = 1,2,\ldots,6216,\ m = 1,2,\ldots,20, \tag{4b}$$

$$\overline{\mathbf{D}}_i(f) = \frac{1}{20}\sum_{m=1}^{20} \mathbf{D}_i(f,m) \quad \in \mathbb{R}^{(6216\times f)}, \tag{4c}$$

$$\text{SVD}(\overline{\mathbf{D}}) = \mathbf{U}\mathbf{S}\mathbf{V}^{\text{T}}, \tag{4d}$$

$$\mathbf{Y} = \mathbf{U}^{\text{T}}\overline{\mathbf{D}} \quad \in \mathbb{R}^{(6216\times f)}, \tag{4e}$$

where $\Im\{.\}$ denotes the imaginary part of the coherence at the ith voxel combination for the mth subject, $\mathbf{U} = [\mathbf{u_1}, \ldots, \mathbf{u_i}] \in \mathbb{R}^{(6216\times6216)}$, $\mathbf{S} \in \mathbb{R}^{(6216\times f)}$ is a pseudo-diagonal matrix consisting of the singular values of $\overline{\mathbf{D}}$ – whose top f rows contains $\mathrm{diag}\{s_1, \ldots, s_f\}$ and whose bottom $(6216 - f)$ rows are zero, $\mathbf{V} = [\mathbf{v_1}, \ldots, \mathbf{v_f}] \in \mathbb{R}^{(f\times f)}$ is the right singular vectors of the contrasted connectivity matrix $\overline{\mathbf{D}}$, and T is the matrix transpose. To determine which of the PLS components are statistically significant, we generated surrogate data using permutation testing (McIntosh and Lobaugh, 2004; Langdon et al., 2011). For each subject, we randomly permuted the connectivity arrays for pre- and post-training before regressing the data against the contrast to obtain subject-level surrogate data. Similar to the original data, the grand-average surrogate spectra were obtained and decomposed into orthogonal components. This analysis was performed for 1000 realizations to estimate the distribution of surrogate components. These surrogate components embody the expected distribution of values under the null hypothesis that there is no training effect (and hence pre- and post-training data are exchangeable). PLS components were considered statistically significant if their eigenvalue exceeded 95% of the corresponding eigenvalues of this surrogate distribution ($p<0.05$). The PLS and statistical analyses rendered three significant components that consistently indicated enhancement in intra-cerebellar and cortico-cerebellar functional connectivity across participants (Figures 4-6).

The significance of the ensuing network edges and their spectral contents was then examined using bootstrapping (McIntosh and Lobaugh, 2004; Langdon et al., 2011). Bootstrapping was performed by randomly permuting the labels of the trials across conditions (pre- and post-training). This generates the null hypothesis that the magnitude of the PLS projections simply reflects finite sample size and noise in the data. Likewise, rejection of the null suggests the presence of a specific training-related change in multivariate functional connectivity measures.

2.7 *Post-hoc analysis*

We then examined the phase relationship and temporal fluctuations of the time-frequency coherence of the edges that were significantly modulated by motor learning. For each significant PLS component, the imaginary part of the time-frequency coherence was averaged across all the significant edges. We then compared the average coherence spectra between pre- and post-training to identify the direction of the changes. In addition, we investigated phase spectra of the significant edges to identify changes in the phase difference between pre- and post-training. We also investigated the temporal fluctuations of the time-frequency coherence by estimating the Hurst component of the temporal fluctuations in coherence for the significant edges and frequencies (Mehrkanoon et al., 2014a). The Hurst exponent quantifies the long-range auto-correlation structure of the time courses of the significant edges in pre- and post- resting-state conditions. We used a two-sample t-test to test whether phase difference and Hurst component of time-frequency coherence were significantly different between pre- and post-motor training.

3 Results

3.1 *Motor skill acquisition*

Significant changes in movement accuracy occurred over the course of the motor training trials, with a clear increase in accuracy but an apparent decrease in movement speed. To test if the improvement in movement accuracy was statistically significant, we partitioned the trials in three blocks: First (6 trials), middle (7 trials), and last (7 trials). A repeated-measures ANOVA revealed a significant decrease in movement error from the first (0.25±0.051 N), middle (0.19±0.04 N) to last block (0.14±0.03 N) ($F(2,19)=2.73$ $p=0.004$; Figure 3A, left panel). In addition to increased movement accuracy, an increase in movement duration was observed across trials: movement duration increase from $\tau = 0.79 \pm 0.12$ s (the first block), $\tau = 0.83 \pm 0.11$ s (the middle block), to $\tau = 1.2 \pm 0.14$ s in the last block. The increase in movement duration was statistically significant ($F(2,19)=10.82$, $p \ll 0.01$; Figure 3A, middle

panel). We also measured the scaling parameter − a parameter that quantifies an interaction between movement-error and movement duration − across the three trial blocks using Eq.1: The scale parameter a increase from 0.9, 1.83 to 2.78 in the first, middle an last block respectively (Figure 3A, right panel). We used bootstrapping to estimate the standard error of the skill and tuning parameters across subjects. We then performed a t-test to compare the skill measure and tuning values across the first and last blocks of trials, which showed the skill parameter significantly increased ($t(19)=6.1$, $p<0.0001$) and the tuning parameter values significantly decreased ($t(19)=-4.1$, $p=0.0003$) between the first and the last block of trials.

These results indicate a speed-accuracy trade-off, as the movement error decrease whilst the movement duration increased (Figure 3B, left panel). Note that the circles, asterisks and triangles correspond to the average movement-error in the three blocks of trials for all 20 participants, respectively (see Figure 3B, left panel). Crucially, participants not only decreased the speed of the cursor movement to obtain greater accuracy, but also exhibited greater accuracy when they performed the cursor movement quickly in the late compared to the early trials. That is, the late trials (triangles) do not only exhibit a reduction in the movement error and an increase in the movement duration, but also show a clear reduction in the movement error at short movement duration − i.e. the early trials (circles) (Figure 3B, left panel). The fitted curves − dashed-line and dotted dashed-line − argue this is true at short times (i.e. $\tau \approx 0.5$ s), but not at longer times: The tail of the fitted curves indeed showed small variability in the movement error at longer movement durations, e.g. $\tau \geq 1.3$ s (Figure 3B, left panel). Importantly, changes in the trend of the fitted curves were captured by the tuning parameter (i.e. rate of task accuracy (Eq.1) across the three blocks of trials: The tuning parameter decreased monotonically from $b = 1.6$ (the first block) to $b = 1.14$ (the middle block) and $b = 0.65$ (the last block) while the movement duration increased (Figure 3B, right panel). Improvement in the performance and accuracy of the cursor movement − i.e. reduction in the movement error with an increase in the movement duration − was associated with a significant effect on the scaling measures that quantified the trade-off between

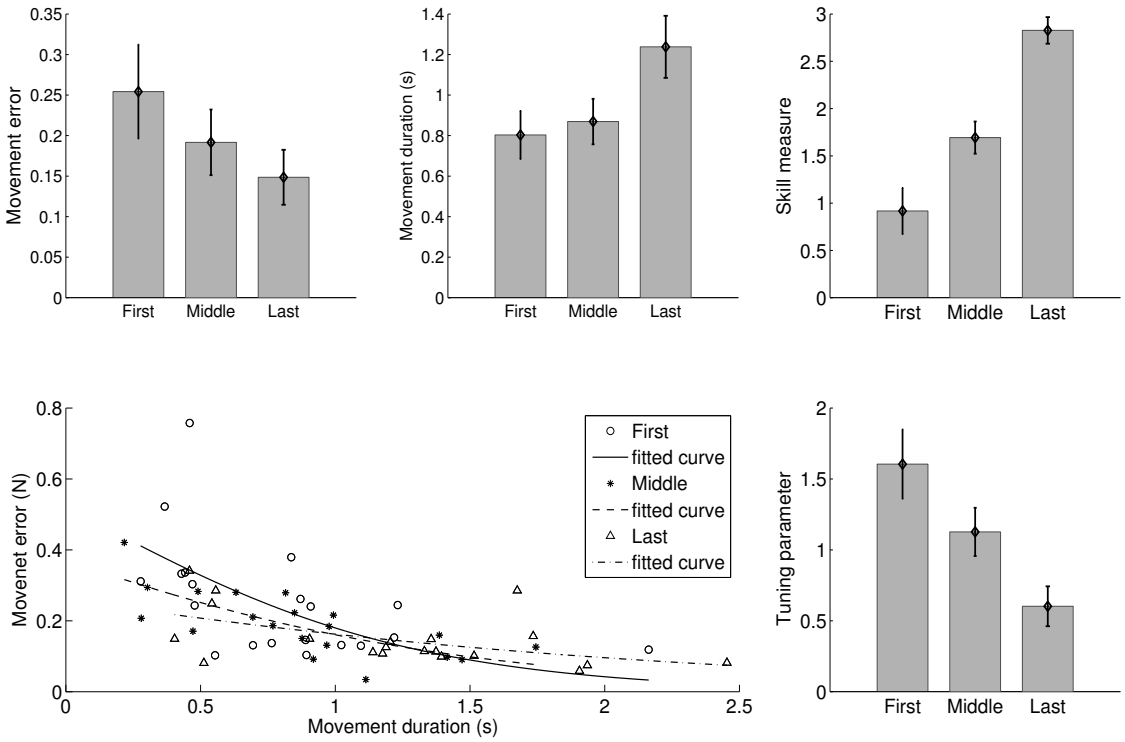

Figure 3: Grand-average motor performance and skill measure in the first- middle- and last- blocks of trials. A) Average movement-error profiles (left panel), average movement duration (middle panel), and skill measure values derived from Eq.(1) (right panel). B) Speed-accuracy trade-off as a function of movement-error and movement duration for the three blocks of trials for all 20 participants (left panel), tuning parameter values for the three block of trials across 20 participants (right panel).

speed and accuracy in the present motor task. This effect suggests that participants changed their strategy (i.e. trajectory planning) over trials from making rapid but inaccurate cursor movements to slower but more accurate movements during a single session of motor training.

3.2 *Cortico-cerebellar functional connectivity*

Following motor training, participants immediately underwent the post resting-state acquisition. Figure 2 recapitulates the steps of the analyses: 1) time-frequency coherence between source time-series captured the linear dependencies between cortical regions (Figure 2C), 2) the PLS of the brain-wide connectivity arrays captured changes in the pre-post resting-state networks (Figure 2D), 3) post-hoc analyses of time-frequency coherence revealed the dynamics of connections that were significantly modulated by motor training (Figure 2E). We found significant differences in the brains intrinsic functional connectivity patterns following motor training. By applying multivariate PLS method to compare pre- and post resting-state connectivity, we identified the connections that were significantly modulated after motor training. The PLS and statistical analyses rendered three significant components ($p<0.01$) that consistently indicated enhancement in intra-cerebellar and cortico-cerebellar functional connectivity across participants (Figure 4−6). Component 1 (15% of the variance, $p=0.02$) showed enhanced functional connectivity between homologous cerebellum areas and between the right precentral (or primary motor cortex) and right postcentral (somatosensory cortex) (Figure 4A−B). Component 2 (9% of the variance, $p=0.03$) showed increased cortico-cerebellar functional connectivity (Figure 5A−B) with connections between precentral and cerebellum regions and with cliques between the left/right cerebellum and vermis. Notably, these cerebellar regions showed increased functional connectivity to left primary motor cortex and right postcentral gyri. These two modes explained 24% of the variance. The third significant component (7% of the variance, $p=0.04$) revealed increased connectivity in a distributed set of connections. These include left and right cerebellar region 6b, left and right temporal pole, right putamen, left and right amygdala, left and right insula and left and right olfactory cortex.

In addition to the connections that were significant modulated due to motor training, PLS also provided the frequency spectra (latent variables) of the connections that were significantly modulated. These spectra showed distinct peaks in the alpha and beta frequency ranges (Figure 7A). Resampling revealed that connectivity was modulated within a few narrow spectral bases indicating narrowband carrier frequencies. Notably, networks 1 and 2 showed a significant ($p<0.05$) peak in the lower mu/alpha frequency (8−11 Hz) and (9−12 Hz) respectively (Figure 7A, left and middle panels), a frequency that is classically characteristic of sensorimotor systems. Network 3 showed two peaks across the lower mu/alpha and the beta range (9−12 Hz) and (19−22 Hz), indicating a large-scale network with narrowband oscillation frequency (right panel). Using post-hoc analyses we then investigated time-frequency coherence of the connections that were significantly modulated by motor training. We first compared the imaginary components of the grand-average coherence spectra: We selected three exemplar pairs of pre- versus post- training significant edges from the three networks shown in Figures 4−6: Left-cerebellum 9−vermis 9 (network 1, Figure 7B, left panel); left primary motor cortex−vermis 3 (network 2, middle panel); and left cerebellum 7b−left temporal mid gyrus (network 3, right panel). The post-training imaginary component of the coherence is more than double the pre-training strength of functional connectivity at the significant frequencies (10 Hz and 20 Hz; $p<0.05$; network 3) such that the pre−post coherence measures are 0.1−0.42 (left panel), -0.03−0.22 (middle panel), -0.05−0.36 and 0.05−0.18 (right panel) respectively. In addition to the strength of coherence, we investigated the phase spectra in order to explore the effect of motor skill acquisition on the phase direction of cerebellum and cortico-cerebellar functional connectivity (Figure 7C). Specifically, we compared the pre and post phase spectra at the specific frequencies found to be significantly different (i.e. 10 Hz and 20 Hz) for the three selected pairs of edges. The post-training phase spectra of the three edges were indeed significantly different ($t_{1,19}=2.72$, $p<0.05$) compared to the pre-training phase spectra. All post-training phase spectra increased compared to the pre phase spectra (row C), indicative of a delay from the cortex to the cerebellum. That is, the cerebellum phase lags the cortex at the carrier frequencies of

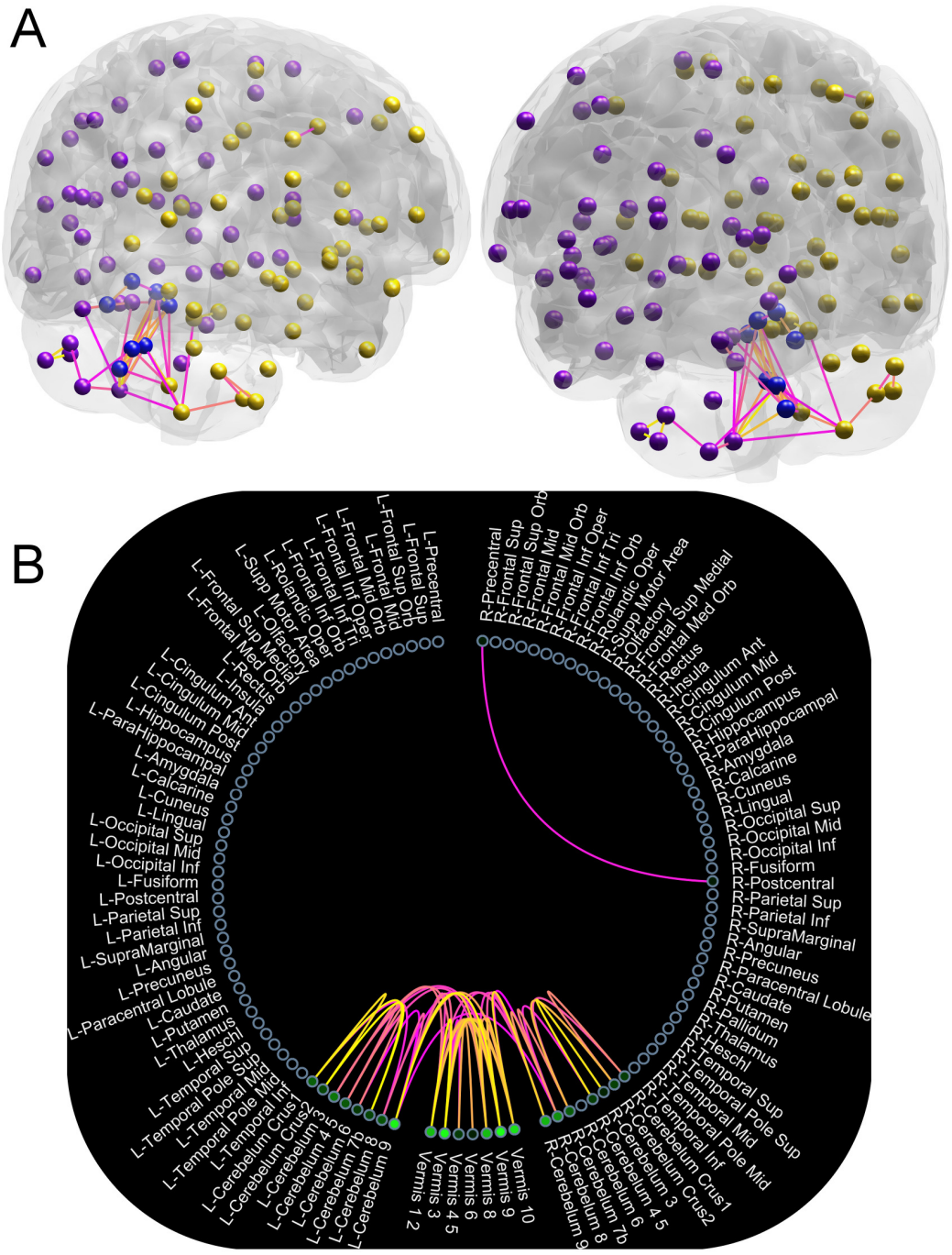

Figure 4: Significant enhancement of resting-state pre-post functional connectivity after motor task performance. A) Increased cerebellum connectivity pattern, and increased connectivity between primary motor cortex and sensorimotor areas, B) topography of functional connectivity in component 1 using a circulogram connectome. The purple, black and yellow voxels (or spheres) represent the Euclidean centers of the ROIs for the left hemisphere, middle (vermis area) and right hemisphere respectively.

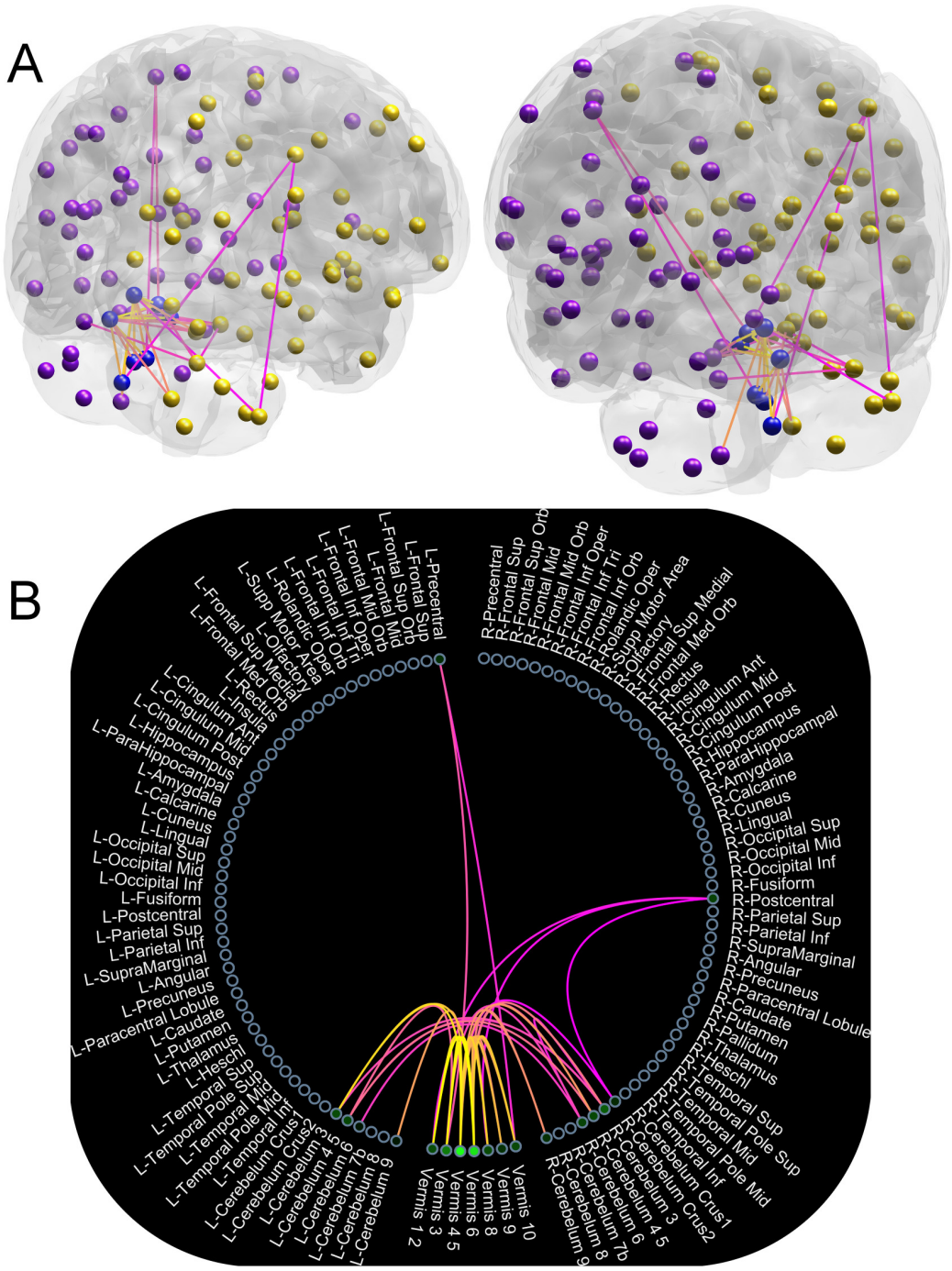

Figure 5: Significant enhancement of resting-state pre-post functional connectivity after motor task performance. A) Increased cortico-cerebellar functional connectivity, B) topography of functional connectivity in component 2 using a circulogram connectome.

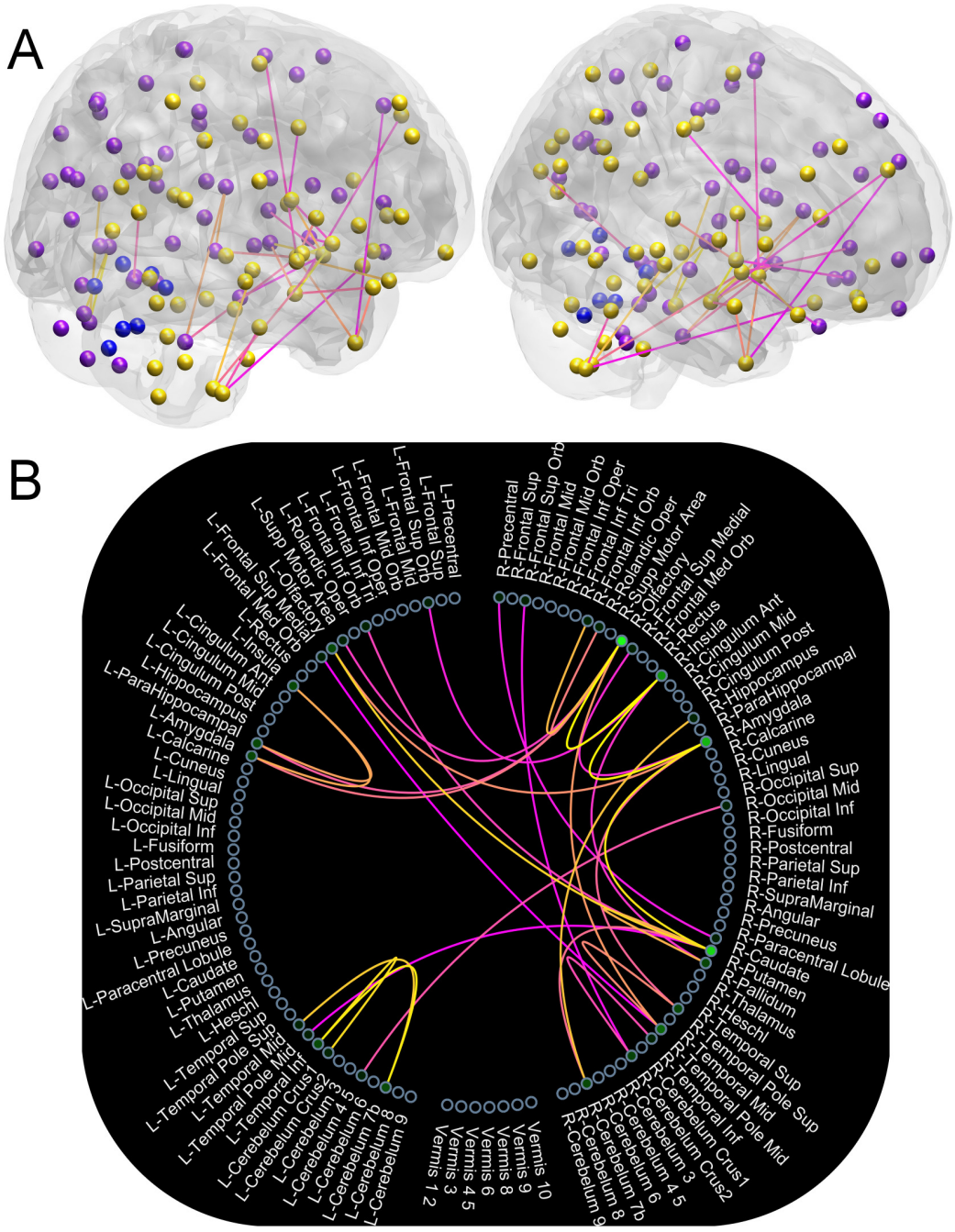

Figure 6: Significant enhancement of resting-state pre-post functional connectivity after motor task performance. A) Increased fronto-temporal connectivity pattern, B) topography of functional connectivity in component 3 using a circulogram connectome.

mu (10 Hz) and beta (20 Hz) bands, indicating the directivity of the effect that accompanies the upregulation of the coherence or synchronization. To illustrate the specificity of these results, we show the functional connectivity for two other edges (right M1 vermis3 and left occipital right parietal) that were not statistically significant (z-score=1.49, p=0.068 and z-score=0.1, p=0.46, respectively; Fig. S1, supplementary material).

Following previous work (Van De Ville et al., 2010; Mehrkanoon et al., 2014a), we finally sought to quantify the temporal evolutions of connectivity in these significant connections using the Hurst exponent. To characterize changes in the dynamics of inter- cerebellum and cortico-cerebellar functional connectivity patterns, we estimated the Hurst exponent of pre- and post-training temporal evolutions of the above three significant edges at significant frequencies 10 Hz (network 1), 11 Hz (network 2), 12 Hz and 20 Hz (net- work 3) (Figure 7D). The mean and standard deviation of the Hurst exponents of the three significant edges obtained from pre and post resting-state conditions lie in the same range 0.58 ± 0.1 and 0.61 ± 0.12 respectively: Left-cerebellum 9-vermis 9 (left panel), left primary motor cortex-vermis 3 (middle panel), and left cerebellum 7b-left temporal mid gyri (right panel). Crucially, the confidence intervals of the Hurst exponent of all networks remain well above 0.5, which implies that the networks have persistent, long-range temporal dependencies consistent with slow power-law decay. The slight increase in these exponents did not reach statistical significance, so only support the persistence of long-range correlations in cortico-cerebellar networks.

We also sought to investigate the power spectral density (PSD) analysis of occipital EEG signals and voxels' signals in the cerebellum to clarify the specificity of the results against potential effects of muscular artifacts on the observed changes in functional connectivity. These analyses revealed limited high-frequency activity indicative of EMG activity. In addition, no significant increase in the spectral power was observed after motor learning that could explain the upregulation of cortico-cerebellar connectivity (Fig. S1D).

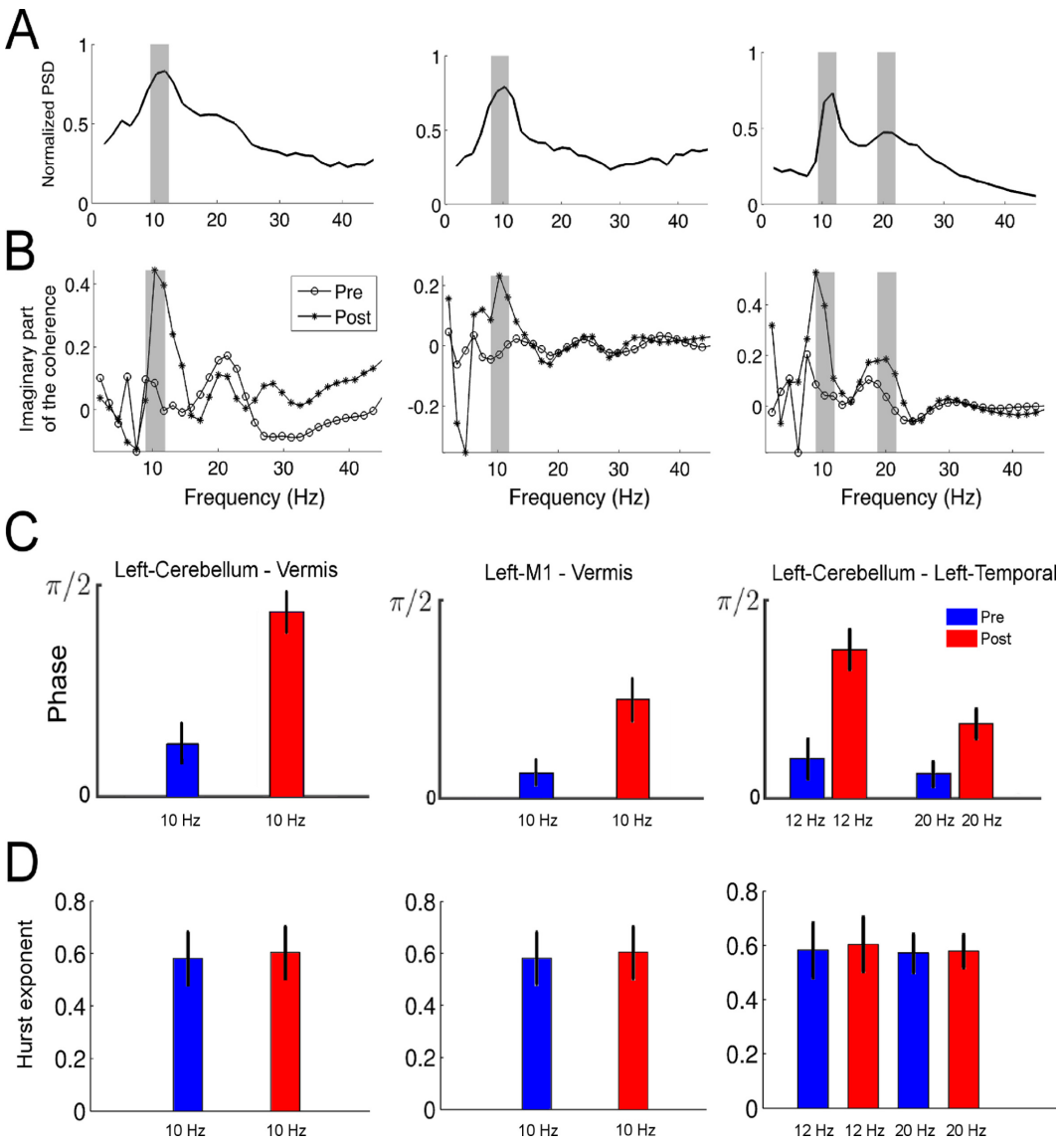

Figure 7: Spectral−temporal dynamics of pre−post resting-state networks. A) Power spectral density of the networks 1, 2 and 3 with peaks at the significant carrier frequencies of 10 Hz (left panel), 11 Hz (middle panel), and 12 Hz, 20 Hz (right panel) respectively, B) the pre and post imaginary parts of the coherence at the significant frequencies (see above) for the three significant edges: Left-cerebellum 9−vermis 9 (component 1) (left panel), left primary motor cortex−vermis 3 (component 2) (middle panel), and left cerebellum 7b−left temporal mid gyrus (component 3) (right panel), C) pre and post phase spectra of the three significant edges at the significant frequencies in component 1 (left panel), component 2 (middle panel), and component 3 (right panel), D) the Hurst exponent of the pre and post temporal evolutions (dynamics) of the three significant edges (see above) from the components 1, 2, and 3 at significant frequencies of 10 Hz (left panel), 11 Hz (middle panel), and 12 Hz and 20 Hz (right panel).

4 Discussion

We investigated changes in cortical and subcortical networks after a single session of motor training, by examining brain-wide functional connectivity in source-reconstructed resting-state EEG. The imaginary part of the coherence was estimated between 112 ROIs during eyes-closed resting-state immediately before and after motor training and changes in brain-wide connectivity induced by motor training were assessed using PLS. We observed three significant components that revealed upregulation in functional connectivity in and between central regions of the motor system, in particularly the cerebellum and motor cortex. These findings are consistent with previous fMRI studies on motor learning (Doyon et al., 2009; Dayan and Cohen, 2011; Hardwick et al., 2013), and hence confirm the feasibility of examining changes in intrinsic connectivity using source-reconstructed EEG. Our analyses additionally reveal that increased coherence was observed in the alpha and beta frequency bands, brain rhythms that have been closely associated with motor control. The corresponding phase spectra revealed greater phase difference after training, indicative of a longer delay from the cortex to the cerebellum. The current results extend previous findings by revealing the changes in synchronous brain oscillations in a distributed motor network following a single session of motor training.

The first two significant PLS components revealed increased connectivity within the cerebellum and between cerebellum and motor cortex. These two modes explained 24 % of the variance. The third mode explained 7% of the variance and revealed increase connectivity in a distributed set of connections including again the cerebellum and the temporal pole, putamen, amygdala and insula. Together these results indicate a prominent role of the cerebellum in the after effects of motor training. The central role of the cerebellum and cortico-cerebellar loops in motor learning are consistent with existent literature (Raymond et al., 1996; Inoue et al., 2000; Della-Maggiore et al., 2009; Nguyen-Vu et al., 2013). Moreover, motor adaptations and learning are impaired in patients with cerebellar damage (Diedrichsen et al., 2005; Smith and Shadmehr, 2005). However, cerebellar activity is tra-

ditionally thought to be difficult to measure using EEG/MEG. The cerebellum is regarded as a deep source, and moreover the dendritic physiology of cerebellar neurons differs from that of pyramidal cells in cerebral cortex. As such, the cerebellum has been generally overlooked in scalp EEG/MEG for several years (Dalal et al., 2013), however, recent studies have further investigated the functional roles of the cerebellum and cortico-cerebellar interactions.

Regions in the cerebellum often exhibit oscillatory activity at much higher frequencies that are not necessarily coherent with other locations (Niedermeyer and da Silva Fernando, 2004). However, when synchrony is imposed on the cerebellar cortex from outside, large-amplitude local field potential (LFP) signals can emerge from cerebellar circuits (Kandel and Buzsáki, 1993; Buzsáki et al., 2012). In addition, the distance between voxels located in the cerebellum and the closest EEG electrodes is between $1-7$ cm, which is similar to the distance between voxels in the occipital cortex and EEG sensors and not as deep as many other subcortical structures. Future work could employ higher-density EEG (128-256 channel caps) together with a realistic head model derived from individual MRIs in order to more accurately identify the cerebellar contributions to cortico-cerebellar functional connectivity in motor learning (Hassan et al., 2014). Indeed, several studies have revealed oscillatory MEG activity originating from the cerebellum in the theta, alpha and beta bands (Gross et al., 2002; Pollok et al., 2009; Jerbi et al., 2007; Fujioka et al., 2012; Dalal et al., 2013). The current findings show increased cerebellar connectivity in the mu/alpha (component 1 and 2) and beta band (component 3), which is consistent with previous studies showing alpha-band coherence in the distributed motor system during sensorimotor integration (Pollok et al., 2009; Gross et al., 2005; Kujala et al., 2007). Given that both the spatial and spectral pattern of increased connectivity observed in this study is consistent with existing literature, these findings confirm the ability to measure cerebellar connectivity using source-reconstructed EEG. To improve electric source imaging analyses, it is hence suggested to use high-density EEG (128-256 channel caps) with realistic head models derived from individual MRIs (Hassan et al., 2014). We examined the PSDs of occipital EEG signals and voxels' signals in the cerebellum to clarify the specificity of the results against the potential effects of muscu-

lar artifacts on the observed changes in functional connectivity (see supplementary material).

We used sLORETA − a distributed dipole model − to reconstruct source activity and computed coherence between all pairs of source signals of 112 anatomically defined ROIs. These analyses resulted in high-dimensional connectivity arrays for the resting-state recording pre and post motor training. Statistical comparison of these connectivity arrays requires controlling the family-wise error rate when mass-univariate testing is performed at every connection comprising the network (Zalesky et al., 2010). Here we use PLS, a multivariate regression technique, to avoid Type-1 errors. Rather than testing every connection separately, PLS extracts consistent changes in coherence across all connections. Permutation testing accommodates the variability between participants. The low number of significant components revealed that while the connectivity arrays were high dimensional, the changes in intrinsic connectivity induced by motor training were in fact low dimensional. That is, the connections that were modulated by motor training revealed similar frequency spectra. PLS hence provides a data-driven approach to map changes in brain-wide connectivity induced by interventions such as motor learning. Wu et al. (2014) also used PLS to identify cortico-cortical coherence in resting-state EEG that was correlated with motor skill acquisition. Whereas they estimated functional connectivity in sensor space and used M1 as seed region, we interrogate brain-wide connectivity in source space. As the method is data driven it can be easily applied to identify changes in intrinsic connectivity induced by other interventions, including brain stimulation techniques such as TMS and tDCS (Polanía et al., 2011; Thut and Miniussi, 2009; Grefkes and Fink, 2011).

Motor performance was assessed by quantifying the speed and accuracy of the force trajectories. In a previous study we showed that cortico-muscular coherence revealed synchronization in the alpha and gamma band only when participants made an overshoot when reaching the second target (Mehrkanoon et al., 2014b). We interpreted this dual-band synchronization as the afferent and efferent processes involved in parsing prediction errors and generating new motor predictions. These prediction errors reflect the mismatch between predicted and

actual sensory outcome of motor commands. In the present study we expected that participants would learn this relationship over time and thereby minimize their prediction error. When comparing speed and accuracy across trials we indeed observed a significant reduction in movement overshoot − and hence increased accuracy − over trials. However movement time also increased across trials. While this trade-off may not indicate increased motor performance per se, it reflects motor adaption as participants adjust their motor commands and the predicted sensory outcomes according to performance on the first few trials, and as revealed by the change in skill measure and tuning parameter (Figure 3).

Interestingly, previous research has shown that sensory prediction errors drive cerebellum-dependent adaption of reaching (Tseng et al., 2007), consistent with the present findings. Motor learning literature broadly distinguishes between motor adaptions and motor sequence learning, as they are mediated by different neural substrates (Doyon et al., 2003). Motor adaption reflects the process by which subjects learn to adapt to environmental perturbations or changes and is primarily mediated by the cortico-cerebellar system (Doyon et al., 2003, 2009; Hardwick et al., 2013). Motor adaptation is generally studied in reaching tasks in which the relationship between movements of a manipulandum and cursor on a monitor is perturbed. While the relationship between forces changes and visual feedback is not perturbed in the presented study, the relationship is still unknown when participants initially commence the task: They hence need to update their internal models while performing this new task (Imamizu et al., 2000). The observed increase in cortico-cerebellar functional connectivity is consistent with this interpretation.

5 Conclusions

The outcomes of the present study indicate that upregulation of cortico-cerebellar network connectivity reflects functional changes as a result of a single session of motor training. Changes in the spectra, phase, and spatiotemporal patterns of source-space EEG resting-state networks reveal that the cerebellum is central in motor adaptions via phase-lagged interactions with the motor cortex and basal ganglia at the mu and beta frequency bands. In sum, using source-reconstruction EEG, we captured the spectral and topographical fingerprints of changes in intrinsic connectivity as a result of motor training. The ability to capture modulations in intrinsic connectivity between the cortex and cerebellum demonstrate the potential of EEG to assess neural plasticity induced by motor training.

Acknowledgements

This work was supported by an Australian Research Council (ARC) Discovery Projects Grant DP130104317 awarded to JJS and MRH.

References

Andrew, D., Yielder, P., Murphy, B., 2015. Do pursuit movement tasks lead to differential changes in early somatosensory evoked potentials related to motor learning compared with typing tasks? Journal of neurophysiology 113 (4), 1156–1164.

Baarbé, J., Yielder, P., Daligadu, J., Behbahani, H., Haavik, H., Murphy, B., 2014. A novel protocol to investigate motor training-induced plasticity and sensorimotor integration in the cerebellum and motor cortex. J. Neurophysiol. 111 (4), 715–721.

Boonstra, T., Daffertshofer, A., Breakspear, M., Beek, P., 2007. Multivariate time-frequency analysis of electromagnetic brain activity during bimanual motor learning. NeuroImage 36 (2), 370–377.

Brookes, M., Woolrich, M., Luckhoo, H., Price, D., Hale, J., Stephenson, M., Barnes, G., Smith, S., Morris, P., 2011. Investigating the electrophysiological basis of resting state networks using magnetoencephalography. Proc. Nat. Acad. Sci. USA 108 (40), 16783–16788.

Brunet, D., Murray, M., Michel, C., 2011. Spatiotemporal analysis of multichannel EEG: Cartool. Comput Intell Neurosci 2011, 1–15.

Buzsáki, G., Anastassiou, C., Koch, C., 2012. The origin of extracellular fields and currents−EEG, ECoG, LFP and spikes. Nature Rev Neurosci 13 (6), 407–420.

Cardoso, J.-F., 1997. Infomax and maximum likelihood for blind source separation. IEEE Signal Process. Lett. 4 (4), 112–114.

Coynel, D., Marrelec, G., Perlbarg, V., Pélégrini-Issac, M., Van de Moortele, P.-F., Ugurbil, K., Doyon, J., Benali, H., Lehéricy, S., 2010. Dynamics of motor-related functional integration during motor sequence learning. NeuroImage 49 (1), 759–766.

Dalal, S., Osipova, D., Bertrand, O., Jerbi, K., 2013. Oscillatory activity of the human cere-

bellum: The intracranial electrocerebellogram revisited. Neuroscience and Biobehavioral Reviews 37 (4), 585–593.

Dayan, E., Cohen, L., 2011. Neuroplasticity subserving motor skill learning. Neuron 72 (3), 443–454.

Deeny, S., Haufler, A., Saffer, M., Hatfield, B., 2009. Electroencephalographic coherence during visuomotor performance: A comparison of cortico-cortical communication in experts and novices. Journal of Motor Behavior 41 (2), 106–116.

Della-Maggiore, V., Scholz, J., Johansen-Berg, H., Paus, T., 2009. The rate of visuomotor adaptation correlates with cerebellar white-matter microstructure. Hum Brain Mapp 30 (12), 4048–4053.

Diedrichsen, J., Verstynen, T., Lehman, S., Ivry, R., 2005. Cerebellar involvement in anticipating the consequences of self-produced actions during bimanual movements. J. Neurophysiol. 93 (2), 801–812.

Doyon, J., Bellec, P., Amsel, R., Penhune, V., Monchi, O., Carrier, J., Lehéricy, S., Benali, H., 2009. Contributions of the basal ganglia and functionally related brain structures to motor learning. Behavioural Brain Research 199 (1), 61–75.

Doyon, J., Benali, H., 2005. Reorganization and plasticity in the adult brain during learning of motor skills. Curr Opin Neurobiol 15 (2), 161–167.

Doyon, J., Penhune, V., Ungerleider, L., 2003. Distinct contribution of the cortico-striatal and cortico-cerebellar systems to motor skill learning. Neuropsychologia 41 (3), 252–262.

Dudai, Y., 2004. The neurobiology of consolidations, or, how stable is the engram? Annu Rev Psychol 55, 51–86.

Floyer-Lea, A., Matthews, P., 2005. Distinguishable brain activation networks for short- and long-term motor skill learning. J. Neurophysiol. 94 (1), 512–518.

Fujioka, T., Trainor, L., Large, E., Ross, B., 2012. Internalized timing of isochronous sounds is represented in neuromagnetic beta oscillations. J Neurosci 32 (5), 1791–1802.

Galea, J., Vazquez, A., Pasricha, N., Orban De Xivry, J.-J., Celnik, P., 2011. Dissociating the roles of the cerebellum and motor cortex during adaptive learning: The motor cortex retains what the cerebellum learns. Cerebral Cortex 21 (8), 1761–1770.

Geladi, P., Kowalski, B., 1986. Partial least-squares regression: a tutorial. Analytica Chimica Acta 185 (C), 1–17.

Grafton, S., Hazeltine, E., Ivry, R., 2002. Motor sequence learning with the nondominant left hand: A pet functional imaging study. Exp. Brain Res. 146 (3), 369–378.

Grefkes, C., Fink, G., 2011. Reorganization of cerebral networks after stroke: New insights from neuroimaging with connectivity approaches. Brain 134 (5), 1264–1276.

Gross, J., Pollok, B., Dirks, M., Timmermann, L., Butz, M., Schnitzler, A., 2005. Task-dependent oscillations during unimanual and bimanual movements in the human primary motor cortex and SMA studied with magnetoencephalography. NeuroImage 26 (1), 91–98.

Gross, J., Timmermann, L., Kujala, J., Dirks, M., Schmitz, F., Salmelin, R., Schnitzler, A., 2002. The neural basis of intermittent motor control in humans. Proc. Nat. Acad. Sci. USA 99 (4), 2299–2302.

Haavik, H., Murphy, B., 2013. Selective changes in cerebellar-cortical processing following motor training. Experimental Brain Research 231 (4), 397–403.

Halsband, U., Lange, R., 2006. Motor learning in man: A review of functional and clinical studies. J. Physiol. Paris 99 (4-6), 414–424.

Hamzei, F., Glauche, V., Schwarzwald, R., May, A., 2012. Dynamic gray matter changes within cortex and striatum after short motor skill training are associated with their increased functional interaction. NeuroImage 59 (4), 3364–3372.

Hardwick, R., Rottschy, C., Miall, R., Eickhoff, S., 2013. A quantitative meta-analysis and review of motor learning in the human brain. NeuroImage 67, 283–297.

Hassan, M., Dufor, O., Merlet, I., Berrou, C., Wendling, F., 2014. Eeg source connectivity analysis: From dense array recordings to brain networks. PLoS ONE 9 (8).

Hikosaka, O., Nakamura, K., Sakai, K., Nakahara, H., 2002. Central mechanisms of motor skill learning. Curr Opin Neurobiol 12 (2), 217–222.

Hipp, J., Hawellek, D., Corbetta, M., Siegel, M., Engel, A., 2012. Large-scale cortical correlation structure of spontaneous oscillatory activity. Nature Neurosci 15 (6), 884–890.

Honda, M., Deiber, M.-P., Ibáñez, V., Pascual-Leone, A., Zhuang, P., Hallett, M., 1998. Dynamic cortical involvement in implicit and explicit motor sequence learning. A PET study. Brain 121 (11), 2159–2173.

Houweling, S., Daffertshofer, A., van Dijk, B., Beek, P., 2008. Neural changes induced by learning a challenging perceptual-motor task. NeuroImage 41 (4), 1395–1407.

Imamizu, H., Miyauchi, S., Tamada, T., Sasaki, Y., Takino, R., Pütz, B., Yoshioka, T., Kawato, M., 2000. Human cerebellar activity reflecting an acquired internal model of a new tool. Nature 403 (6766), 192–195.

Inoue, K., Kawashima, R., Satoh, K., Kinomura, S., Sugiura, M., Goto, R., Ito, M., Fukuda, H., 2000. A PET study of visuomotor learning under optical rotation. NeuroImage 11 (5 I), 505–516.

Jerbi, K., Lachaux, J.-P., N'Diaye, K., Pantazis, D., Leahy, R., Garnero, L., Baillet, S., 2007. Coherent neural representation of hand speed in humans revealed by MEG imaging. Proc. Nat. Acad. Sci. USA 104 (18), 7676–7681.

Kandel, A., Buzsáki, G., 1993. Cerebellar neuronal activity correlates with spike and wave EEG patterns in the rat. Epilepsy Res 16 (1), 1–9.

Karni, A., Meyer, G., Jezzard, P., Adams, M., Turner, R., Ungerleider, L., 1995. Functional MRI evidence for adult motor cortex plasticity during motor skill learning. Nature 377 (6545), 155–158.

Karni, A., Meyer, G., Rey-Hipolito, C., Jezzard, P., Adams, M., Turner, R., Ungerleider, L., 1998. The acquisition of skilled motor performance: Fast and slow experience- driven changes in primary motor cortex. Proc. Nat. Acad. Sci. USA 95 (3), 861–868.

Karni, A., Sagi, D., 1993. The time course of learning a visual skill. Nature 365 (6443), 250–252.

Kelly, A., Garavan, H., 2005. Human functional neuroimaging of brain changes associated with practice. Cerebral Cortex 15 (8), 1089–1102.

Krakauer, J., Mazzoni, P., 2011. Human sensorimotor learning: Adaptation, skill, and beyond. Curr Opin Neurobiol 21 (4), 636–644.

Krishnan, A., Williams, L., McIntosh, A., Abdi, H., 2011. Partial least squares (pls) methods for neuroimaging: A tutorial and review. NeuroImage 56 (2), 455–475, cited By 118.

Kujala, J., Pammer, K., Cornelissen, P., Roebroeck, A., Formisano, E., Salmelin, R., 2007. Phase coupling in a cerebro-cerebellar network at 8-13 Hz during reading. Cerebral Cortex 17 (6), 1476–1485.

Langdon, A., Boonstra, T., Breakspear, M., 2011. Multi-frequency phase locking in human somatosensory cortex. Prog Biophys Mol Biol 105 (1-2), 58–66.

Lehéricy, S., Benali, H., Van De Moortele, P.-F., Pélégrini-Issac, M., Waechter, T., Ugurbil, K., Doyon, J., 2005. Distinct basal ganglia territories are engaged in early and advanced motor sequence learning. Proc. Nat. Acad. Sci. USA 102 (35), 12566–12571.

Luft, A., Buitrago, M., 2005. Stages of motor skill learning. Mol Neurobiol 32 (3), 205–216.

Ma, L., Narayana, S., Robin, D., Fox, P., Xiong, J., 2011. Changes occur in resting state network of motor system during 4 weeks of motor skill learning. NeuroImage 58 (1), 226–233.

Mantini, D., Perrucci, M., Del Gratta, C., Romani, G., Corbetta, M., 2007. Electrophysiological signatures of resting state networks in the human brain. Proc. Nat. Acad. Sci. USA 104 (32), 13170–13175.

Mazziotta, J., Toga, A., Evans, A., Fox, P., Lancaster, J., Zilles, K., Woods, R., Paus, T., Simpson, G., Pike, B., Holmes, C., Collins, L., Thompson, P., MacDonald, D., Iacoboni, M., Schormann, T., Amunts, K., Palomero-Gallagher, N., Geyer, S., Parsons, L., Narr, K., Kabani, N., Le Goualher, G., Boomsma, D., Cannon, T., Kawashima, R., Mazoyer, B., 2001. A probabilistic atlas and reference system for the human brain: International consortium for brain mapping (ICBM). Phil. Trans. R. Soc. B 356 (1412), 1293–1322.

McIntosh, A., Lobaugh, N., 2004. Partial least squares analysis of neuroimaging data: Applications and advances. NeuroImage 23 (SUPPL. 1), S250–S263.

Mehrkanoon, S., Breakspear, M., Boonstra, T., 2014a. Low-dimensional dynamics of resting-state cortical activity. Brain Topogr 27 (3), 338–352.

Mehrkanoon, S., Breakspear, M., Boonstra, T., 2014b. The reorganization of corticomuscular coherence during a transition between sensorimotor states. NeuroImage 100, 692–702.

Mehrkanoon, S., Breakspear, M., Britz, J., Boonstra, W., 2014c. Intrinsic coupling modes in source-reconstructed intrinsic coupling modes in source-reconstructed electroencephalography. Brain Connectivity 4 (10), 812–825.

Mehrkanoon, S., Breakspear, M., Daffertshofer, A., Boonstra, T. W., 2013. Non-identical smoothing operators for estimating time-frequency interdependence in electrophysiological recordings. EURASIP J ADV SIG PR 2013 (73), 1–16.

Nguyen-Vu, T., Kimpo, R., Rinaldi, J., Kohli, A., Zeng, H., Deisseroth, K., Raymond, J.,

2013. Cerebellar purkinje cell activity drives motor learning. Nature Neurosci 16 (12), 1734–1736.

Niedermeyer, E., da Silva Fernando, H. L., 2004. Electroencephalography: Basic Principles, Clinical Applications, and Related Fields. Lippincot Williams & Wilkins.

Nolte, G., Bai, O., Wheaton, L., Mari, Z., Vorbach, S., Hallett, M., 2004. Identifying true brain interaction from EEG data using the imaginary part of coherency. Clin Neurophysiol 115 (10), 2292–2307.

Pascual-Leone, A., Amedi, A., Fregni, F., Merabet, L., 2005. The plastic human brain cortex. Annu. Rev. Neurosci. 28, 377–401.

Pascual-Marqui, R., 2002. Standardized low-resolution brain electromagnetic tomography (sloreta): Technical details. Methods and Findings in Experimental and Clinical Pharmacology 24 (SUPPL. D), 5–12.

Polanía, R., Nitsche, M., Paulus, W., 2011. Modulating functional connectivity patterns and topological functional organization of the human brain with transcranial direct current stimulation. Human Brain Mapping 32 (8), 1236–1249.

Pollok, B., Krause, V., Butz, M., Schnitzler, A., 2009. Modality specific functional interaction in sensorimotor synchronization. Hum Brain Mapp 30 (6), 1783–1790.

Pollok, B., Latz, D., Krause, V., Butz, M., Schnitzler, A., 2014. Changes of motor-cortical oscillations associated with motor learning. Neuroscience 275, 47–53.

Raymond, J., Lisberger, S., Mauk, M., 1996. The cerebellum: A neuronal learning machine? Science 272 (5265), 1126–1131.

Reis, J., Schambra, H., Cohen, L., Buch, E., Fritsch, B., Zarahn, E., Celnik, P., Krakauer, J., 2009. Noninvasive cortical stimulation enhances motor skill acquisition over multiple days through an effect on consolidation. Proc. Nat. Acad. Sci. USA 106 (5), 1590–1595.

Sakai, K., Hikosaka, O., Miyauchi, S., Sasaki, Y., Fujimaki, N., Pütz, B., 1999. Presupplementary motor area activation during sequence learning reflects visuo-motor association. J Neurosci 19 (10).

Sami, S., Robertson, E., Chris Miall, R., 2014. The time course of task-specific memory consolidation effects in resting state networks. J Neurosci 34 (11), 3982–3992.

Sanes, J., Donoghue, J., 2000. Plasticity and primary motor cortex. Annu. Rev. Neurosci. 23, 393–415.

Smith, M., Shadmehr, R., 2005. Intact ability to learn internal models of arm dynamics in huntington's disease but not cerebellar degeneration. J. Neurophysiol. 93, 2809–2821.

Taubert, M., Lohmann, G., Margulies, D., Villringer, A., Ragert, P., 2011. Long-term effects of motor training on resting-state networks and underlying brain structure. NeuroImage 57 (4), 1492–1498.

Thut, G., Miniussi, C., 2009. New insights into rhythmic brain activity from tms-eeg studies. Trends in Cognitive Sciences 13 (4), 182–189.

Tomassini, V., Jbabdi, S., Kincses, Z., Bosnell, R., Douaud, G., Pozzilli, C., Matthews, P., Johansen-Berg, H., 2011. Structural and functional bases for individual differences in motor learning. Hum Brain Mapp 32 (3), 494–508.

Tropini, G., Chiang, J., Wang, Z., Ty, E., McKeown, M., 2011. Altered directional connectivity in parkinson's disease during performance of a visually guided task. NeuroImage 56 (4), 2144–2156.

Tung, K.-C., Uh, J., Mao, D., Xu, F., Xiao, G., Lu, H., 2013. Alterations in resting functional connectivity due to recent motor task. NeuroImage 78, 316–324.

Tzvi, E., Münte, T., Krämer, U., 2014. Delineating the cortico-striatal-cerebellar network in implicit motor sequence learning. NeuroImage 94, 222–230.

Ungerleider, L., Doyon, J., Karni, A., 2002. Imaging brain plasticity during motor skill learning. Neurobiol Learn Mem 78 (3), 553–564.

Vahdat, S., Darainy, M., Milner, T., Ostry, D., 2011. Functionally specific changes in resting-state sensorimotor networks after motor learning. J Neurosci 31 (47), 16907–16915.

Van De Ville, D., Britz, J., Michel, C., 2010. EEG microstate sequences in healthy humans at rest reveal scale-free dynamics. Proc. Nat. Acad. Sci. USA 107 (42), 18179–18184.

Wu, J., Srinivasan, R., Kaur, A., Cramer, S., 2014. Resting-state cortical connectivity predicts motor skill acquisition. NeuroImage 91, 84–90.

Zalesky, A., Fornito, A., Bullmore, E., 2010. Network-based statistic: Identifying differences in brain networks. NeuroImage 53 (4), 1197–1207.